第41卷第1期
2022年2月

红外与毫米波学报
J. Infrared Millim. Waves

Vol. 41, No. 1
February,2022

文章编号：1001-9014(2022)01-0279-06

DOI:10. 11972/j. issn. 1001-9014. 2022. 01. 022

Influence of oxygen partial pressure on the optical properties of β-$Ga_2O_{3-\delta}$ films deposited by pulsed laser deposition

LI Liu-Meng[1], ZHOU Bin[1], GAO Li-Chen[1], JIANG Kai[1], ZHU Liang-Qing[1], ZHANG Jin-Zhong[1*], HU Zhi-Gao[1,2,3*], CHU Jun-Hao[1,2,3]

(1. Technical Center for Multifunctional Magneto-Optical Spectroscopy (Shanghai), Engineering Research Center of Nanophotonics & Advanced Instrument (Ministry of Education), Department of Materials, School of Physics and Electronic Science, East China Normal University, Shanghai 200241, China;
2. Collaborative Innovation Center of Extreme Optics, Shanxi University, Taiyuan 030006, China;
3. Shanghai Institute of Intelligent Electronics & Systems, Fudan University, Shanghai 200433, China)

Abstract: High quality β-$Ga_2O_{3-\delta}$ films on *c*-sapphire substrates are deposited by pulsed laser deposition (PLD) under various oxygen partial pressures. The crystalline structure, chemometry and optical properties of the β-$Ga_2O_{3-\delta}$ films are investigated systematically by X-ray diffraction (XRD), far-infrared reflectance spectra, X-ray photoelectron spectroscopy (XPS) and ultraviolet-visible-near infrared (UV-vis-NIR) transmittance spectra. The XRD analysis shows that all the as-deposited films are of unique (-201) orientation. The transmittance spectra reveal that the films exhibit a high transparency above 80% in the UV-vis-NIR wavelength region above 255 nm (4. 863 eV). Moreover, the optical constants and optical direct bandgap are extracted based on the transmittance spectra with Tauc-Lorentz (TL) dispersion function model and Tauc's relationship, respectively. A further step, the influence of oxygen partial pressure on optical properties is explained by theoretical calculation.

Key words: β-Ga_2O_3, pulsed laser deposition, oxygen partial pressure, optical properties

氧分压对脉冲激光沉积β-$Ga_2O_{3-\delta}$薄膜光学性能的影响

李留猛[1]，周 斌[1]，高立宸[1]，姜 凯[1]，朱亮清[1]，张金中[1*]，胡志高[1,2,3*]，褚君浩[1,2,3]

(1. 华东师范大学 物理与电子科学学院,材料科学系,纳光电集成与先进装备教育部工程研究中心,
上海市极化材料多功能磁光光谱技术服务平台,上海 200241;
2. 山西大学 极端光学协同创新中心,山西 太原 030006;
3. 复旦大学 上海智能电子与系统研究院,上海 200433)

摘要:在不同氧分压下,用脉冲激光沉积法在*c*-蓝宝石衬底上制备了高质量β-$Ga_2O_{3-\delta}$薄膜。通过X-射线衍射、远红外反射光谱、X-射线光电子能谱和紫外-可见-近红外透射光谱系统地研究了β-$Ga_2O_{3-\delta}$薄膜的晶格结构、化学计量比和光学性质。X-射线衍射分析表明,所有沉积的薄膜以(-201)晶向方向生长。透射光谱显示薄膜在255 nm以上的紫外-可见-近红外波段具有80%以上的高透明度,同时在255 nm附近有一个陡峭的吸收边。此外,利用Tauc-Lorentz (TL)色散函数模型和Tauc公式,我们提取了β-$Ga_2O_{3-\delta}$薄膜的光学常数和光学直接带隙。更进一步,我们通过理论计算解释了氧气分压对β-$Ga_2O_{3-\delta}$薄膜光学性质的影响。

关 键 词:氧化镓;脉冲激光沉积;氧分压;光学性质

中图分类号:O484.1　　**文献标识码**:A

Received date: 2021-07-06, **revised date**: 2021-09-06　　**收稿日期**:2021-07-06,**修回日期**:2021-09-06

Foundation items: Supported by the National Key R&D Program of China (2018YFB0406500 and 2019YFB2203400); the Natural Science Foundation of China (91833303, 61974043, 62074058, 62090013 and 61974044); Projects of Science and Technology Commission of Shanghai Municipality (18JC1412400, 18YF1407200, 18YF1407000 and 19511120100); the Program for Professor of Special Appointment (Eastern Scholar) at Shanghai Institutions of Higher Learning and Shanghai Pujiang Program (20PJ1403600).

Biography: LI Liumeng (1994-), male, Shanghai, Ph. D, Research area involves gallium oxide materials and devices. E-mail: 52181213020@stu.ecnu.edu.cn

[*] **Corresponding authors**: E-mail: jzzhang@ee.ecnu.edu.cn, zghu@ee.ecnu.edu.cn

Introduction

Gallium oxide (Ga_2O_3) has five polymorphs: α, β, γ, δ and ε[1-3]. When heated to a certain temperature, all other phases are converted to the monoclinic β-phase, which is the most stable structure[4-5]. As an ultra wide bandgap oxide semiconductor (~4.9 eV), β-Ga_2O_3 exhibits better optical properties and high breakdown electrical field (~8×10^6 V/cm)[6-8]. Therefore, gallium oxide has great application prospects in gas sensors, solar-blind ultraviolet photodetectors, electroluminescent devices, high power devices and other electronic devices[9-12]. In addition, β-Ga_2O_3 can be used as a window on some types of optical devices due to the high optical transparency below its optical bandgap[1]. Gallium oxide films can be prepared by metal-organic chemical vapor deposition[2,13], molecular beam epitaxy[14], radio frequency sputtering[15], atomic layer deposition[16], sol-gel[17], and pulsed laser deposition (PLD)[18-19]. Among these methods, PLD has its unique advantages: i) it can keep the composition of deposited films and target consistent; ii) it can control the oxygen vacancies in gallium oxide film by adjusting the oxygen partial pressure; iii) it can be used to grow single crystal films at low temperature and low vacuum; iv) it has strong flexibility and a fast growth speed, which could satisfy the needs of previous research on gallium oxide films.

Deposition of gallium oxide films by PLD has been reported by other research groups. Wang *et al.* reported the effects of deposition temperatures on the performance of gallium oxide films for optoelectronic devices. They finally realized the β-Ga_2O_3 based solar-blind detectors with a good performance of a low dark current (10.6 pA) at 10 V and a high peak responsibility (18.23 A/W) at 255 nm[20]. For PLD deposition of β-Ga_2O_3 films, oxygen partial pressure, deposition time, laser power and substrate types are essential for the quality of the as-deposited films besides deposition temperature[21-23]. Under different oxygen partial pressures, oxygen vacancies at gallium oxide films will change, resulting in the variations on optical constants and bandgap. This change can be extracted from the transmission spectra in the ultraviolet-visible-near infrared (UV-vis-NIR) wavelength range.

In this work, the β-Ga_2O_3 films on *c*-sapphire have been deposited by PLD under different oxygen partial pressures. It is found that the films exhibit a high transparency above 80% in the UV-vis-NIR wavelength region above 255 nm. The influences of oxygen partial pressure on optical properties such as optical constants and optical bandgap have been discussed in detail. The results are helpful to develop the application of Ga_2O_3-based photodetectors.

1 Experiments

Gallium oxide films were deposited on *c*-sapphire substrates by PLD under various oxygen partial pressures (P_O = 5, 10, 20, and 40 mTorr). First, sapphire substrates were cleaned by acetone, ethanol, and deionized water for 5 mins in an ultrasonic cleaning bath before deposition. Gallium oxide target was synthesized by gallium oxide powder with a purity of 99.9%. Then, the *c*-sapphire substrates were heated to 700 °C. A pulsed KrF laser (248 nm) with the energy density of 2.6 mJ/cm^2 was used at a repetition rate of 10 Hz and the deposition time was 1 h. The pressure in the vacuum chamber was less than 5×10^{-4} mTorr, and high purity oxygen (99.999%) was passed into the cavity as active gas. Note that the holder was rotated to deposit a uniform film. The effect of oxygen partial pressure on gallium oxide films has been systematically studied. The structural characteristics of gallium oxide films were analyzed by X-ray diffraction (XRD, Bruker D8 Advance diffractometer) with a Cu Kα radiation λ = 1.541 8 Å at room temperature. The far-infrared (FIR) reflectance spectra in the wavenumber range of 50-700 cm^{-1} were recorded by Bruker VERTEX 80V FTIR spectrometer. X-ray photoelectron spectroscopy (XPS, RBD-upgraded PHI-5000C ESCA system, PerkinElmer) with a Mg Kα radiation ($h\nu$ = 1 253.6 eV) was used to analyze the stoichiometries and valence states of elements in the as-grown $Ga_2O_{3-\delta}$ films. The UV-vis-NIR transmission spectra were measured with a double-beam ultraviolet-infrared spectrophotometer (PerkinElmer Lambda 950) in the photon wavelength range from 200 nm to 1 000 nm (1.24~6.2 eV) with a step of 2 nm. The transmission spectra were fitted by the Tauc-Lorentz model, and the absorption edge and optical constants of β-Ga_2O_3 films on *c*-sapphire substrates were obtained, which are consistent with the theoretical prediction.

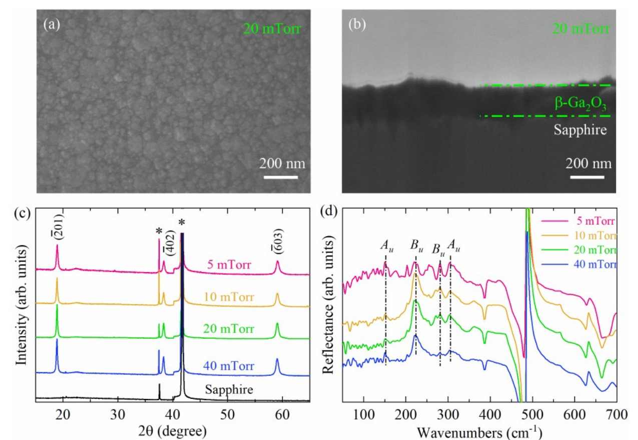

Fig. 1 (a) Plane-view and (b) cross-sectional SEM images of a β-$Ga_2O_{3-\delta}$ film deposited under the oxygen partial pressure of 20 mTorr, and (c) XRD patterns of the as-grown β-$Ga_2O_{3-\delta}$ films on *c*-sapphire substrates deposited under various oxygen partial pressures from 5 to 40 mTorr, the peaks labelled by the symbol (*) come from the sapphire substrates, (d) FIR reflectance spectra of the $Ga_2O_{3-\delta}$/*c*-sapphire samples. The dashed lines indicate the transverse optical (TO) infrared active phonon modes. Note that the curves are shifted vertically for clarity

图1 在20mTorr氧分压下制备的β-$Ga_2O_{3-\delta}$薄膜样品的(a)表面和(b)界面SEM图,(c) 5~40mTorr不同氧分压下,在c-蓝宝石衬底上生长的β-$Ga_2O_{3-\delta}$薄膜的X-射线衍射谱,(d) β-$Ga_2O_{3-\delta}$/c-蓝宝石样品的远红外反射光谱,虚线表示横向光学(TO)红外活性声子模式,为了清晰,在y方向上对光谱进行了平移

2 Results and discussions

As an example, the plane-view and cross-sectional microstructure of the $Ga_2O_{3-\delta}$ film deposited under the oxygen partial pressure of 20 mTorr are shown in Fig. 1(a) and 1(b), respectively. It suggests that the film surface is smooth and its thickness is about 200 nm. Fig. 1(c) shows the XRD patterns of gallium oxide films deposited on *c*-sapphire substrates under different oxygen partial pressure of 5, 10, 20 and 40 mTorr. It reveals that all the spectra have obvious characteristic peaks nearby 18.9, 38.4, 41.9, and 59.1°. The peak at around 41.9° originates from the *c*-sapphire substrate, corresponding to the (0006) plan[24]. The peaks nearby 18.9, 38.4, and 59.1° are assigned to (-201), (-402) and (-603) planes of β-Ga_2O_3, respectively. It indicates that the polycrystalline monoclinic β-Ga_2O_3 films with high quality are grown with the (-201) preferred orientation (JCPDF No. 41-1103)[20]. Fig. 1(d) displays the FIR reflectance spectra in the wavenumber range of 50-700 cm^{-1}. There are three obvious reflection bands, which are located at around 150, 220, and 303 cm^{-1}, respectively. According to the prediction of group theory about β-Ga_2O_3: $\Gamma_{opt} = 10A_g(Raman) + 5B_g(Raman) + 4A_u(IR) + 8B_u(IR)$[25-26], the IR-spectra of the samples are very similar to those of monoclinic system. The reflection band of 150.4 cm^{-1} is the $A_u(TO_1)$ vibration mode, which is corresponding to the upward and downward movement of gallium ions. The $B_u(TO_1)$ one nearby 219.8 cm^{-1} arises from the scissor's movement of Ga-O-Ga. The $A_u(TO_2)$ vibration (302.8 cm^{-1}) is related to a symmetrical Ga-O-Ga stretching[26-27]. Note that the phonon frequencies are almost the same for the β-$Ga_2O_{3-\delta}$ films deposited under various oxygen pressures, while the related intensities of $B_u(TO_1)$ and $A_u(TO_2)$ have an obvious difference. It means the Ga-O-Ga related lattice dynamics and crystalline structure are affected by the oxygen partial pressure.

The survey XPS spectra of the four gallium oxide films on *c*-sapphire substrates were measured, which have a similar feature. As an example, Fig. 2(a) shows the survey XPS of the β-$Ga_2O_{3-\delta}$ films deposited under the oxygen partial pressure of 5 mTorr. The experimental results were calibrated with the C 1s peak at 284.5 eV. The strong peaks come from Ga 3d, Ga 3p, Ga 3s, Ga 2p, Ga LMM Auger peak, O 1s, C 1s and O KLL[28]. The appearance of the carbon peak can be ascribed to the adsorption of amorphous carbon pollutants on the film surface[29]. However, no aluminum peaks were observed, indicating that the substrate ions do not diffuse into β-$Ga_2O_{3-\delta}$. The XPS spectra contain peaks of O, Ga, and C without other elements, which indicate that the purity of the deposited gallium oxide films is high. The fine scanning spectra and fitted results from Ga 2p and O 1s peaks are depicted in Fig. 2(b) and Fig. 2(c), respectively. The relative atomic ratio and bonding phase of the surface region were calculated by Shirley iterative method and linear function based on the asymmetric shape analysis of Ga 2p and O 1s spectra. The Gaussian-Lorentzian mixture function is used to simulate the experimental spectra by the program XPSPEAK4.1.

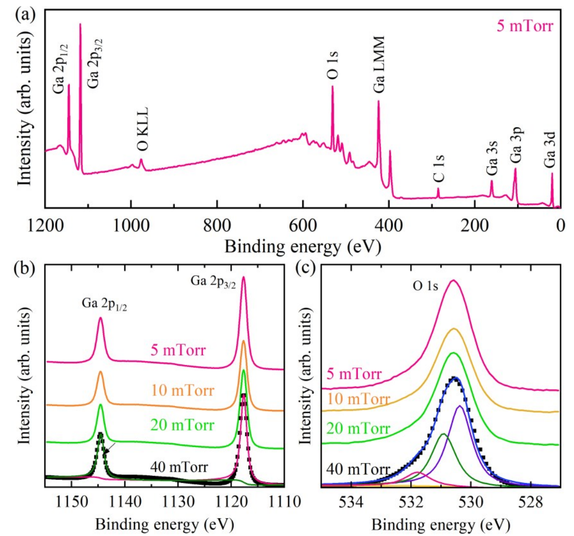

Fig. 2 (a) The survey XPS spectra of β-$Ga_2O_{3-\delta}$ films deposited under the oxygen pressure of 5 mTorr, the experimental and best-fitted XPS fitting results of the (b) Ga 2p and (c) O 1s peaks for samples deposited under the various oxygen pressures of 5, 10, 20, and 40 mTorr

图2 (a)在5 mTorr氧压下沉积的β-$Ga_2O_{3-\delta}$薄膜的光电子能谱,(b)在不同氧压(5,10,20和40 mTorr)下沉积的样品的Ga 2p和(c)O 1s峰的实验和最佳拟合结果

Fig. 2(b) shows that Ga 2p exhibits two sub peaks (Ga $2p_{1/2}$ and Ga $2p_{3/2}$) nearby 1145 and 1118 eV, respectively. The fitting results suggest that the peaks have a shift to high binding energy from 1144.52 to 1144.55 eV for Ga $2p_{1/2}$ and 1117.65 to 1117.68 eV for Ga $2p_{3/2}$ with increasing the oxygen pressure. Fig. 2(c) shows the XPS fitting results of the O 1s nuclear level spectra. The O 1s peak can be fitted to be composed of the Ga-O bond of Ga_2O_3 at the binding energy of 530.37~531.45 eV, the O-H bond nearby 531.79~531.87 eV and oxygen vacancies at around 530.91~531.11 eV. It indicates that O 1s peaks come from Ga_2O_3, oxygen vacancy and O-H, and shift to higher binding energy as the oxygen partial pressure increases. Many factors, such as charge transfer effect, electric field, hybridization and environmental charge density, could cause the shift of binding energy. Among these factors, charge transfer effect plays an important role[30]. Finally, we obtained Ga:O ratio values of the β-$Ga_2O_{3-\delta}$ films deposited under the oxygen partial pressures of 5, 10, 20 and 40 mTorr, which are 2:2.614, 2:2.658, 2:2.670, and 2:2.714, respectively.

In Fig. 3(a), the UV-vis-NIR transmission spectra of β-$Ga_2O_{3-\delta}$ films deposited under various oxygen partial pressures can be divided into a transparent area in the visible region and an intensely absorbing area in the ultraviolet region. The transmittance of all the films in the vis-NIR range is above 80%, indicating that the films have good optical transmittance. Moreover, there is a sharp absorption edge nearby 255 nm (4.863 eV). According to the well-known Tauc relationship[31]: $(\alpha E)^2 \propto (E-E_g)$, the direct optical bandgap (E_g) decreases from 4.96 to 4.90 eV as the oxygen partial pressure increases from 5 to 40 mTorr, as shown in Fig. 3(b). Note that

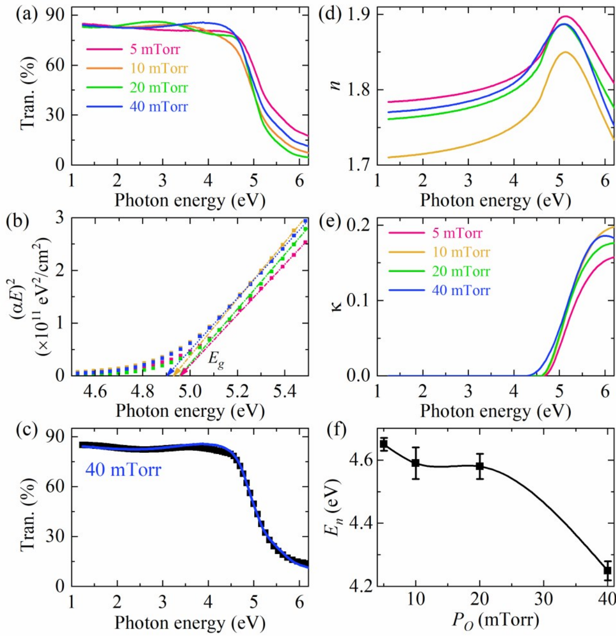

Fig. 3 (a) Transmittance spectra of the β-$Ga_2O_{3-\delta}$/*c*-sapphire samples deposited under the oxygen partial pressures of 5, 10, 20, and 40 mTorr, (b) the plots of $(\alpha E)^2$ as a function of photon energy for direct bandgap, the arrows indicate the optical bandgap of β-$Ga_2O_{3-\delta}$ films, (c) experimental (dotted lines) and best-fitted (solid lines) transmittance spectra of a β-$Ga_2O_{3-\delta}$ film under the oxygen partial pressure of 40 mTorr, (d) refractive index *n* and (e) extinction coefficient *κ* of the β-$Ga_2O_{3-\delta}$ films deposited at various oxygen partial pressures, (f) the extracted absorption edge as a function of oxygen partial pressure

图3 (a)在5，10，20，and 40 mTorr氧分压下沉积的β-$Ga_2O_{3-\delta}$/c-蓝宝石样品的透射光谱，(b)(αE)2作为直接带隙光子能量的函数，箭头表示β-$Ga_2O_{3-\delta}$薄膜的光学带隙，(c)在40 mTorr氧气分压下沉积的β-$Ga_2O_{3-\delta}$薄膜的实验(虚线)和最佳拟合(实线)透射光谱，(d)在不同氧分压下沉积的β-$Ga_2O_{3-\delta}$薄膜的折射率n和(e)消光系数κ，(f)提取的吸收边和氧分压的函数关系

the trend is agreeing with that derived by the Tauc-Lorentz dispersion model (cf. Table 1).

In order to extract the fundamental optical parameters of gallium oxide films, the transmission spectra are analyzed by using a multilayer model (void/film/sapphire). The structure model was constructed under the hypothesis that the films grown on the substrates were treated as isotropic materials. Furthermore, the electron transitions between energy bands can be expressed by dispersion functions. The dielectric functions can be derived by the Tauc-Lorentz (TL) dispersion model, which originates from the standard Lorentz form for the imaginary part ε_2 of a collection of noninteracting atoms and the Tauc joint density of states. The TL model is extensively used to many amorphous and crystalline materials from transparent to strong absorption regions[32-33]. The imaginary part of the TL dispersion function is

$$\varepsilon_2(E)=\begin{cases}\dfrac{AE_0C(E-E_n)^2}{(E^2-E_0^2)^2+C^2E^2}\cdot\dfrac{1}{E}, E>E_g\\ 0, E\leqslant E_g\end{cases} . \quad (1)$$

The real part (ε_1) is derived from the Kramers-Kronig relation:

$$\varepsilon_1(E)=\varepsilon_\infty+\frac{2}{\pi}P\int_{E_g}^{\infty}\frac{\xi E_2(\xi)}{\xi^2-E^2}d\xi \quad , \quad (2)$$

where A is the transition matrix element, E_0 is the peak position energy, C is the broadening term, E_n is the electronic transition energy, and ε_∞ is the high frequency dielectric constant. The appropriate value of ε_∞ depends on the dispersion model at lower energies. So, ε_∞ is fixed to a certain value ($\varepsilon_\infty=1$) for all films in order to reduce the number of parameters and enhance the comparison between different films. For example, the experiment (dotted lines) and best-fitted (solid lines) spectra for the sample (P_o = 40mTorr) are shown in Fig. 3(c). The optimized parameter (electronic transitions, film thickness, etc.) values of the TL model are summarized in Table1. The derived optical constants ($\tilde{n}=n+ik=\sqrt{\tilde{\varepsilon}}=\sqrt{\varepsilon_1+i\varepsilon_2}$) as a function of photon energy are shown in Fig. 3(d) and 3(e), respectively. In the visible-near ultraviolet region, the refractive index n increases with increasing photon energy and the extinction coefficient k is nearby zero due to the lower absorption. In the higher photon energy region above 4.5 eV, the refractive index n reaches a maximum at around 5.2 eV and the extinction coefficient k increases rapidly with increasing photon energy, indicating that the occurrence of interband transitions. These phenomena suggest that it can be used in the field of ultraviolet photodetect[34-36]. In addition, the extracted thickness values of β-$Ga_2O_{3-\delta}$ films are various between 124 and 202 nm, which is in accordance with the results of SEM (Fig. 1b). The absorption edge is various from 4.65 to 4.25 eV, as depicted in Fig. 3(f). It reveals that the oxygen partial pressure can affect film deposition speed and absorption edge/bandgap.

Table 1 Parameter values of the Tauc−Lorentz model for the $Ga_2O_{3-\delta}$ films determined from the simulation of transmittance spectra

表1 Tauc−Lorentz模型拟合$Ga_2O_{3-\delta}$薄膜的透射光谱的参数值

Samples	P_O (mTorr)	A (eV)	E_0 (eV)	C (eV)	E_n (eV)	Thickness (nm)
#1	5	69.94 (6.43)	4.65 (0.07)	1.93 (0.08)	4.65 (0.02)	124 (1)
#2	10	23.91 (3.93)	5.39 (0.07)	2.11 (0.2)	4.59 (0.05)	168 (3)
#3	20	61.82 (6.60)	4.88 (0.34)	2.08 (0.27)	4.58 (0.04)	202 (3)
#4	40	63.78 (6.60)	4.75 (0.46)	1.96 (0.25)	4.25 (0.06)	143 (5)

To further understand the mechanism of optical properties of the as-deposited β-$Ga_2O_{3-\delta}$ films, the first-principles calculations were performed based on the density functional theory (DFT), using the projector augmented-wave method as implemented in the Vienna Ab *initio* Simulation Package (VASP) code[37-38]. A plane-

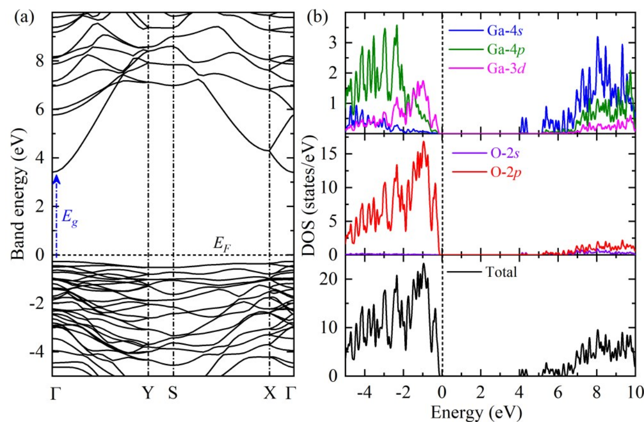

Fig. 4 (a) Band structure and (b) partial and total density of states (DOS) of intrinsic β-Ga_2O_3
图4 本征的β-Ga_2O_3的(a)能带结构和(b)部分和总的态密度

wave basis set with a cutoff of 350 eV and a *k*-mesh of 5×5×5 were adopted to sample the first Brillouin zone. The conjugate gradient scheme is used for the geometric optimization until the force on each atom is less than 0.01 eV/Å, and the total energy change is less than 10^{-6}eV to acquire good convergence. The electronic properties of β-Ga_2O_3 are calculated using the HSE06 methods with a mixing exchange parameter of 0.25 and a screening parameter of 0.2 $Å^{-1}$. The calculated band structure and density of states (DOS) of the intrinsic β-Ga_2O_3 are plotted in Figs. 4(a) and 4(b), respectively. The bandgap of β-Ga_2O_3 in our calculation result is above 3.67 eV, and both the valence band maximum (VBM) and conduction band minimum (CBM) are situated at the Γ point. It means the intrinsic β-Ga_2O_3 is direct bandgap semiconductor, which is suitable for the application of optoelectronic devices[39]. The band structure of β-Ga_2O_3 exhibits a very flat valence band, indicating a large hole effective mass and leading to a low hole mobility. From the partial DOS results, the CBM of the intrinsic β-Ga_2O_3 is formed mainly by Ga-3*d* states, in which the VBM is mainly composed by the O-2*p*, Ga-4*p* and Ga-4*d* states. Therefore, the variation in optical bandgap of the as-deposited β-$Ga_2O_{3-δ}$ films originates from the VBM tuned by the oxygen partial pressure.

3 Conclusions

In conclusion, a series of monoclinic β-$Ga_2O_{3-δ}$ films on *c*-sapphire substrates were deposited by PLD under the oxygen partial pressure range of 5 mTorr to 40 mTorr. XPS results indicate that the Ga∶O ratio approaches to the ideal value (2∶3) as the oxygen partial pressure increases. The influence of oxygen partial pressure on optical constants (refractive index *n* and extinction coefficient *k*), electronic transitions, and thickness of the as-deposited films were extracted by fitting transmittance spectra using the TL dispersion model. In particular, the optical bandgap is various with different partial oxygen pressures due to the change of the valence band maximum, which is mainly composed by O-2p, Ga-4p and Ga-4d states. It has been found that the optimum value of oxygen partial pressure is around 20 mTorr. This work provides comprehensive support to the β-Ga_2O_3 based opto-electronic applications.

References

[1] PEARTON S J, YANG J, CARY P H, *et al*. A view of Ga_2O_3 materials, processing, and device [J]. *Applied Physics Reviews*, 2018, **5** (1): 011301.
[2] XIA X, CHEN Y, FENG Q, *et al*. Hexagonal phase-pure wide band gap ε-Ga_2O_3 films grown on 6H-SiC substrates by metal organic chemical vapor deposition [J]. *Applied Physics Letters*, 2016, **108** (20): 202103.
[3] ROY R, HILL V, OSBORN E. Polymorphism of Ga_2O_3 and the system Ga_2O_3-H_2O [J]. *Journal of the American Chemical Society*, 1952, **74**(3): 719-722.
[4] HIGASHIWAKI M, SASAKI K, KURAMATA A, *et al*. Gallium oxide (Ga_2O_3) metal-semiconductor field-effect transistors on single-crystal β-Ga_2O_3(010) substrates [J]. *Applied Physics Letters*, 2012, **100**(1): 013504.
[5] GELLER S. Crystal structure of β-Ga_2O_3 [J]. *The Journal of Chemical Physics*, 1960, **33**(3): 676.
[6] NAGARAJAN L, DE SOUZA R A, SAMUELIS D, *et al*. A chemically driven insulator-metal transition in non-stoichiometric and amorphous gallium oxide [J]. *Nature Materials*, 2008, **7**: 391-398.
[7] ZHOU H, ZHANG J, ZHANG C, *et al*. A review of the most recent progresses of state-of-art gallium oxide power devices [J]. *Journal of Semiconductors* 2015, **40**(1): 011803.
[8] CHEN X H, REN F F, GU S L, *et al*. Review of gallium-oxide-based solar-blind ultraviolet photodetectors [J]. *Photonics Research*, 2019, **7**(4): 381-415.
[9] CHIKOIDZE E, FELLOUS A, PEREZ-TOMAS A, *et al*. P-type β-gallium oxide: A new perspective for power and optoelectronic devices [J]. *Materials Today Physics*, 2017, **3**: 118-126.
[10] PANG R, TERAMURA K, TATSUMI H, *et al*. Modification of Ga_2O_3 by an Ag-Cr core-shell cocatalyst enhances photocatalytic CO evolution for the conversion of CO_2 by H_2O [J]. *Chemical Communications*, 2018, **54**(9): 1053-1056.
[11] LIN R C, ZHENG W, ZHANG D, *et al*. High-performance graphene/β-Ga_2O_3 heterojunction deep-ultraviolet photodetector with hot-electron excited carrier multiplication [J]. *ACS Applied Materials & Interfaces*, 2018, **10**(26): 22419-22426.
[12] YOO J H, RAFIQUE S, LANGE A, *et al*. Lifetime laser damage performance of β-Ga_2O_3 for high power applications [J]. *APL Materials*, 2018, **6**(3): 036105.
[13] CAO Q, HE L, XIAO H, *et al*. β-Ga_2O_3 epitaxial films deposited on epi-GaN/sapphire (0001) substrates by MOCVD [J]. *Materials Science in Semiconductor Processing*, 2018, **77**: 58-63.
[14] KRACHT M, KARG A, SCHORMANN J, *et al*. Tin-assisted synthesis of ε-Ga_2O_3 by molecular beam epitaxy [J]. *Physical Review Applied*, 2017, **8**(5): 054002.
[15] MAHMOUD W E. Solar blind avalanche photodetector based on the cation exchange growth of β-Ga_2O_3/SnO_2 bilayer heterostructure thin film [J]. *Solar Energy Materials and Solar Cells*, 2016, **152**: 65-72.
[16] NAM T, LEE C W, KIM H J, *et al*. Growth characteristics and properties of Ga-doped ZnO (GZO) thin films grown by thermal and plasma-enhanced atomic layer deposition [J]. *Applied Surface Science*, 2014, **295**: 260-265.
[17] KOKUBUN Y, MIURA K, ENDO F, *et al*. Sol-gel prepared β-Ga_2O_3 thin films for ultraviolet photodetectors [J]. *Applied Physics Letters*, 2007, **90**(3): 031912.
[18] MATSUZAKI K, YANAGI H, KAMIYA T, *et al*. Field-induced current modulation in epitaxial film of deep-ultraviolet transparent oxide semiconductor Ga_2O_3 [J]. *Applied Physics Letters*, 2006, **88**(9): 092106.
[19] FENG Q, LI F, DAI B, *et al*. The properties of gallium oxide thin film grown by pulsed laser deposition [J]. *Applied Surface Science*, 2015, **359**: 847-852.
[20] WANG Q, CHEN J, HUANG P, *et al*. Influence of growth temperature on the characteristics of β-Ga_2O_3 epitaxial films and related solar-blind photodetectors [J]. *Applied Surface Science*, 2019, **489**: 101-109.
[21] CHOI W, SANDS T. Effect of oxygen partial pressure during pulsed laser deposition on the orientation of CeO_2 thin films grown on (100) silicon [J]. *Journal of Materials Research*, 2003, **18**(8): 1753-

1756.
[22] OUJJA M, REBOLLAR E, QUESADA A, *et al*. Effect of wavelength, deposition temperature and substrate type on cobalt ferrite thin films grown by pulsed laser deposition [J]. *Applied Surface Science*, 2018, **452**(15): 19-31.
[23] AL-BUSAIDY M S, KUSMARTSEVA O E, CRAPPER M D. Pulsed laser deposition of metallic multilayers: the influence of laser power on microstructure [J]. *Applied Physics A*, 2004, **79**(4): 1453-1456.
[24] ZHANG F, SAITO K, TANAKA T, *et al*. Structural and optical properties of Ga_2O_3 films on sapphire substrates by pulsed laser deposition [J]. *Journal of Crystal Growth*, 2014, **387**:96-100.
[25] LIU B, GU M, LIU X. Lattice dynamical, dielectric, and thermodynamic properties of β-Ga_2O_3 from first principles [J]. *Applied Physics Letters*, 2007, **91**(17): 172102.
[26] SCHUBERT M, KORLACKI R, KNIGHT S, *et al*. Anisotropy, phonon modes, and free charge carrier parameters in monoclinic β-gallium oxide single crystals [J]. *Physical Review B*, 2016, **93**(12): 125209.
[27] VILLORA E G, MORIOKA Y, ATOU T, *et al*. Infrared reflectance and electrical conductivity of β-Ga_2O_3 [J]. *Physica Status Solidi A*, 2002, **193**(1): 187-195.
[28] SHI F, QIAO H. Effects of hydrothermal temperatures on crystalline quality and photoluminescence properties of β-Ga_2O_3 microspheres using ammonia as a precipitator [J]. *CrystEngComm*, 2021, **23**(2): 492-498.
[29] RAMACHANDRAN R K, DENDOOVEN J, BOTTERMAN J, *et al*. Plasma enhanced atomic layer deposition of Ga_2O_3 thin films [J]. *Journal of Materials Chemistry A*, 2014, **2**(45): 19232-19238.
[30] CHU L, LIN T, HUANG M, *et al*. Ga_2O_3(Gd_2O_3) on Ge without interfacial layers: Energy-band parameters and metal oxide semiconductor devices [J]. *Applied Physics Letters*, 2009, **94**(20): 202108.
[31] CHIKOIDZE E, SARTEL C, MOHAMED H, *et al*. Enhancing the intrinsic p-type conductivity of the ultra-wide bandgap Ga_2O_3 semiconductor [J]. *Journal of Materials Chemistry C*, 2019, **7**(33): 10231-10239.
[32] JELLISON JR. G E J, MODINE F A. Parameterization of the optical functions of amorphous materials in the interband region [J]. *Applied Physics Letters*, 1996, **69**(3): 371-373.
[33] SEGEV D, WEI S-H. Structure-derived electronic and optical properties of transparent conducting oxides [J]. *Physical Review B*, 2005, **71**(12): 125129.
[34] HWANG W S, VERMA A, PEELAERS H, *et al*. High-voltage field effect transistors with wide-bandgap β-Ga_2O_3 nanomembranes [J]. *Applied Physics Letters*, **104**(20): 203111.
[35] KIM J, OH S, MASTRO M A, *et al*. Exfoliated β-Ga_2O_3 nano-belt field-effect transistors for air-stable high power and high temperature electronics [J]. *Physical Chemistry Chemical Physics*, 2016, **18**(23): 15760- 15764.
[36] OH S, KIM J, REN F, *et al*. Quasi-two-dimensional β-gallium oxide solar-blind photodetectors with ultrahigh responsivity [J]. *Journal of Materials Chemistry C*, 2016, **4**(39): 9245-9250.
[37] ZHOU B, JIANG K, SHANG L, *et al*. Enhanced carrier separation in ferroelectric In_2Se_3/MoS_2 van der Waals heterostructure [J]. *Journal of Materials Chemistry C*, 2020, **8**(32): 11160-11167.
[38] KRESSE G, HAFNER J. Ab initio molecular-dynamics simulation of the liquid-metal-amorphous semiconductor transition in germanium [J]. *Physical Review B*, 1994, **49**(20): 14251-14269.
[39] HE H, ORLANDO R, BLANCO M A, *et al*. First-principles study of the structural, electronic, and optical properties of Ga_2O_3 in its monoclinic and hexagonal phases [J]. *Physical Review B*, 2006, **74**(19): 195123.